# Biomolecular dynamic covalent polymers for DNA complexation and siRNA delivery

Camille Bouillon, Yannick Bessin, Florian Poncet, Magali Gary-Bobo, Pascal Dumy, Mihail Barboiu, Nadir Bettache, Sébastien Ulrich

Journal of Materials Chemistry B

PAPER

# Biomolecular Dynamic Covalent Polymers for DNA complexation and siRNA delivery

Received 00th January 20xx,
Accepted 00th January 20xx

DOI: 10.1039/x0xx00000x

www.rsc.org/

Camille Bouillon,[a] Yannick Bessin,[a] Florian Poncet,[a] Magali Gary-Bobo,[a] Pascal Dumy,[a] Mihail Barboiu,[b] Nadir Bettache*[a] and Sébastien Ulrich*[a]

Synthetic delivery systems that are described as smart are considered essential for the successful development of gene therapies. Dynamic covalent polymers (DCP) are dynamic and adaptive species that can expand and shorten their main chain in a reversible fashion. In particular, polyacylhydrazone DCPs are pH-sensitive and undergo hydrolytic dissociation at acidic pH, which is an interesting feature for gene delivery. Building upon our previous finding that cationic DCPs can complex DNA through multivalent interactions, we report here on a new generation of DCPs that incorporate modified amino acids. The covalent self-assembly through polycondensation was extended towards multifunctional DCPs combining different building blocks and different molecular dynamics. These biomolecular DCPs were found able to complex both long DNA and siRNA, and biological studies demonstrate that they are able to deliver functional siRNA in living cells. This straightforward and modular approach to the self-production of multifunctional and biomolecular DCPs as siRNA vectors can therefore constitute a stepping stone in smart gene delivery using dynamic and adaptive biodynamers.

## Introduction

Gene therapies such as antisense,[1, 2] siRNA,[3] and CRISPR-Cas9[4] technologies have opened up tremendous medical perspectives. However, their translation to the clinic has not yet been effective, and the delivery of therapeutic oligonucleotides still remains a major issue.[5] Although viral vectors are very effective, they continue to pose serious toxicity threats.[6] As a result, artificial non-viral vectors are very much needed.[7-9]

Cationic polymers have been very instrumental as a first generation of synthetic vectors but present two major limitations: i) their non-degradability results in their accumulation in living tissues which causes toxic side-effects, and ii) their strong complexation to oligonucleotides due to multivalent interactions prevent an effective release.[10-12] Currently, there is therefore a strong interest in designing "smart" artificial vectors that self-assemble, adapt to the presence of the target and/or to the barriers to cross during the delivery process, and release oligonucleotides in a controlled manner with a concomitant degradation of the vector into non-toxic smaller fragments that can be eliminated more easily.[13-24]

Dynamic covalent polymers,[25-31] which have already found interest in material science for their self-healing properties, are strong candidates for such biological application and should be considered as "smart" polymer therapeutics.[32] Unlike standards polymers which are stable and constitutionally static structures, dynamic covalent polymers result from the dynamic self-assembly of their main-chain through multiple reversible covalent bonds. Interestingly, the control over their growth and decay may be very useful to tune the multivalent interactions commonly at play in oligonucleotide complexation and cell penetration.

A number of recent works has pushed toward this grand challenge of controlling oligonucleotide recognition with dynamic covalent polymers, using mainly two types of chemical linkages: disulfides which are redox-sensitive,[33-35] and acylhydrazones which are pH-sensitive.[36, 37] For instance, Matile *et al.* have developed Cell-Penetrating polyDisulfides (CPD) that self-assemble through a ring-opening polymerization and degrade under intracellular reductive conditions or by a reaction with free thiols present on cell membranes.[38-46] Aida *et al.* have also worked on polydisulfides and interestingly demonstrated the templating role of the DNA target on the polymerization process, yielding a vector that is best adapted to its target and able to transfect siRNA in cells.[47] Our groups have previously developed linear Dynamic Covalent Polymers (DCPs)[48] and branched Dynamic Covalent Frameworks (DCFs)[49-52] that spontaneously self-assemble their linear or dendritic main-chains from simple building blocks and exert a strong binding to DNA due to multivalent interactions. Furthermore, our polyacylhydrazone DCPs were found to be dynamic, undergoing cycle–chain interconversion depending on the concentration, and degradable in a pH-dependent

[a] IBMM, Université de Montpellier, CNRS, ENSCM, UM, Montpellier, France. E-mail : nadir.bettache@umontpellier.fr; Sebastien.Ulrich@enscm.fr
[b] IEM, Adaptive Supramolecular Nanosystems Group, Université de Montpellier, CNRS, ENSCM, UM, Montpellier, France

Electronic Supplementary Information (ESI) available: [detailed materials and methods, synthetic protocols and additional characterization data]. See DOI: 10.1039/x0xx00000x

manner – their hydrolytic depolymerization being faster at acidic pH (pH = 4-5, similar to typical pH found in tumor tissues and late endosomes compartments) than at neutral pH. Recently, such modular covalent self-assembly through acylhydrazones enabled Montenegro *et al.* to identify self-assembled peptide amphiphiles bearing dynamic side-chains for the delivery of plasmids,[53] siRNA,[54] and Cas9.[55]

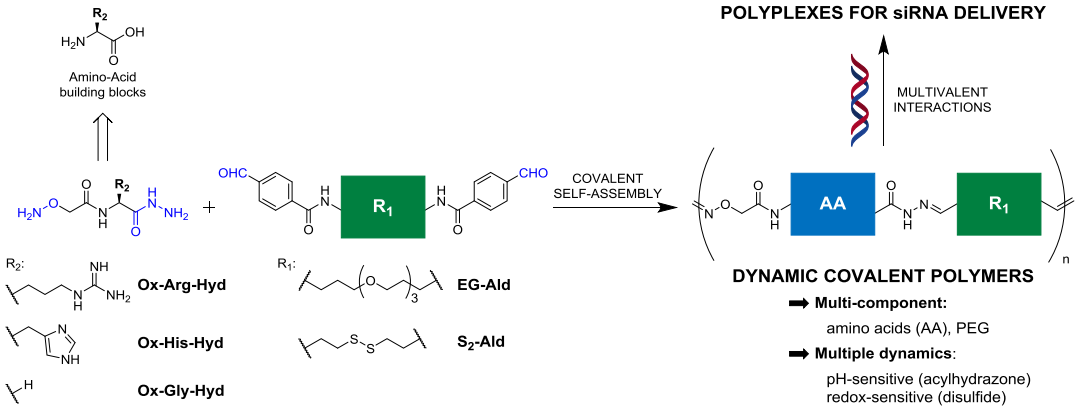


**Fig. 1** Modular covalent self-assembly of multi-component Dynamic Covalent Polymers from modified amino acids through a polycondensation process involving acylhydrazone and oxime reactions.

Besides displaying controlled dynamic features, the self-assembled artificial gene delivery vectors of the future will most likely be multi-component in order to combine the different properties required (oligonucleotide complexation, cell penetration – ideally targeted to certain cell types –, and endosomal escape),[56, 57] and will also feature multiple dynamics.[58] Such a design is expected to reveal synergistic effects that should be beneficial to the delivery process.[59, 60] However, to date, such systems are essentially made from synthetic building blocks. It is therefore of interest to develop alternative approaches using readily-available biomolecules as feed-stock in order to expand the scope of DCPs.

We report herein a modular synthetic strategy that extends DCPs toward multi-functional biopolymers (Fig. 1). Specifically, we introduce modified amino acids that are combined with synthetic bisaldehydes in order to yield biomolecular DCPs. Biological studies show that they act as effective siRNA delivery vectors in living cells.

## Results and discussion

### Strategy

The covalent self-assembly of complementary bisfunctionalized building blocks yield alternate DCPs. Poly-acylhydrazones are thus typically produced through a polycondensation between a bisaldehyde and a bishydrazide.[48, 61] Similarly, poly-oximes are generated from bisaldehydes and bisaminooxy building blocks.[62, 63]

Although synthetic methods allow the introduction of aldehyde groups into peptides,[64] it is often easier to introduce hydrazide and aminooxy groups. For instance, a hydrazide function can be readily created at the C-terminal by standard peptide coupling reactions – carried out either in solution or through solid-phase peptide synthesis – using a protected hydrazine as nucleophile.[65] The attachment of a hydrazide group at the N terminal can be more problematic.[66] On the other hand, aminooxy groups can be readily appended at the N-terminal end of aminoacids and peptides by using readily-available activated esters such as compound **4** (Scheme 1) bearing a protected aminooxy function. Therefore, we decided to introduce into DCPs amino acids featuring a hydrazide and an aminooxy group at, respectively, the C- and N-termini, thus forming a novel class of "Molecular Biodynamers".[67] We expected that these **Ox-AA-Hyd** building blocks would undergo both acylhydrazone and oxime ligations in mild conditions.[68, 69] Whereas the latter would be essentially irreversible in those conditions, the former is well known for its reversibility endowing dynamic and adaptive features to DCPs, as well as its pH-sensitivity that is of great interest for drug and gene delivery applications.

### Synthesis of modified amino acids Ox-AA-Hyd

We focused first on inserting cationic amino acids (Fig. 2) for imparting affinity for DNA through electrostatic interactions. Indeed, the guanidinium group (pKa ≈ 13) of Arginine is very effective for promoting the interaction with the DNA phosphodiesters through salt-bridge interactions, in a typical effect coined "Arginine magic".[15] On the other hand, the imidazole group of Histidine is a weaker base (pKa ≈ 6) which results in polyhistidines being usually less protonated at physiological conditions than polyarginines. While this can be detrimental for promoting DNA complexation, such incorporation of multiple histidines can be beneficial for activating a proton-sponge-type endosomal escape while keeping a good complexation efficacy.[70-75] Finally, Glycine was also tested as a neutral control compound.

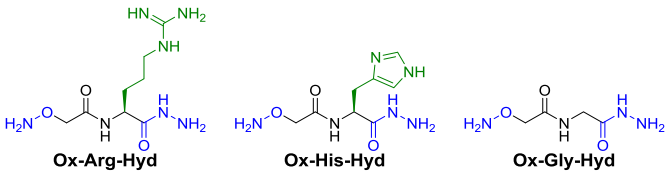


**Fig. 2** Structures of amino acid building blocks **Ox-AA-Hyd** derived from, from left to right, Arginine, Histidine, and Glycine.

The preparation of these amino acid derivatives was carried out as described in Scheme 1. While a standard Fmoc strategy in solution was employed for the synthesis of **Ox-Arg-Hyd** and

**Ox-His-Hyd**, it proved less appropriate for **Ox-Gly-Hyd** due to difficulties in the purification and isolation of compound **2a**. In the end, a Cbz strategy was found to be successful for obtaining this product. The commercially available protected amino acids were engaged in a coupling reaction with *tert*-butylcarbazate mediated by (EDC) / (HOBt) to afford the compounds **1a**-**1c** in good yields (92% to quantitative yields). Then the protected group on the N-terminal of the amino acids hydrazide were removed, by hydrogenation with 10% Pd/C (for compound **1a**) or by reaction with piperidine in dimethylformamide (for compounds **1b** and **1c**), to give the corresponding amines **2a**-**2c** (84% to quantitative yields). The next step was the introduction of the protected oxyamine group by coupling the activated *N*-hydrosuccinimmide ester with the amines **2a**-**2c** in presence of diisopropylethylamine (DIEA) to provide the compounds **3a**-**3c** (75%-87% yield). Finally the deprotection of all protecting groups was achieved using TFA/TIS/$H_2O$ (95:2.5:2.5) and yielded the desired **Ox-AA-Hyd** compounds.

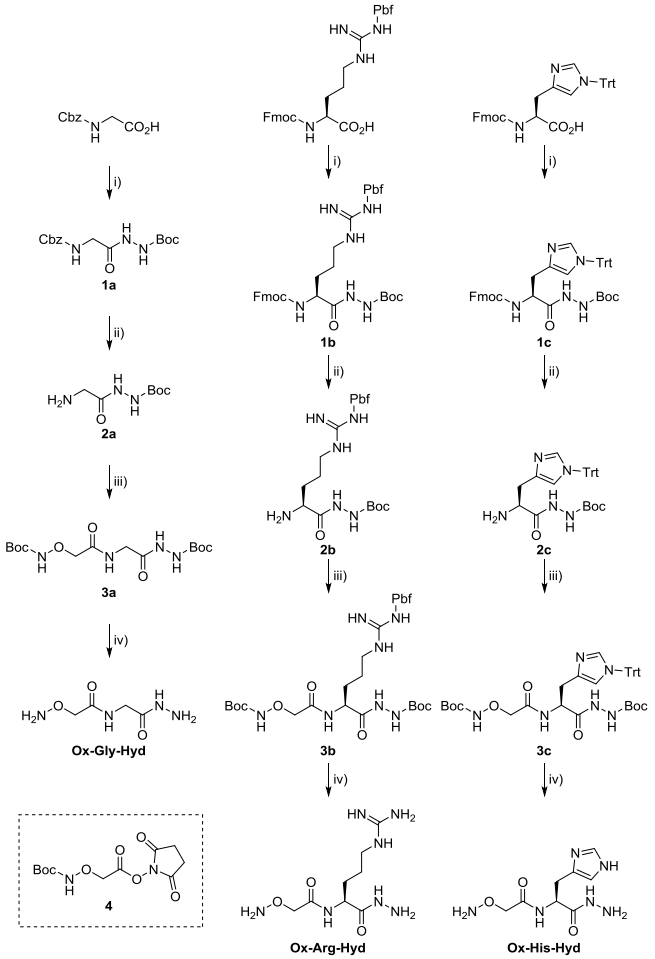


**Scheme 1** Synthesis of amino acid building blocks Ox-AA-Hyd. Reagents and conditions: i) *tert*-butylcarbazate, EDC, HOBt, $Et_3N$, $CH_2Cl_2$ 0° to rt; ii) $H_2$/Pd/C, MeOH, rt for **1a** and DMF/piperidine (8/2), rt for **1b** and **1c**; iii) **4**, DIEA, $CH_2Cl_2$, rt; iv) TFA/TIS/$H_2O$ (95/2.5/2.5), rt.

### Synthesis of bisaldehydes

The bisaldehyde building block containing a triethylene glycol spacer, **EG-ALD** (Fig. 3), was synthesized as previously reported by our group.[48] We also report here the introduction of a disulfide linkage into the bisaldehyde component (compound **$S_2$-ALD**, Fig. 3). This bioreducible linkage is often used in the design of smart gene delivery vectors and we were particularly interested in combining, within the same DCP, this redox-sensitive linkage with the pH-sensitive acylhydrazones.

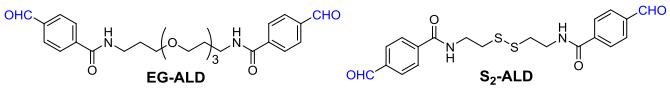


**Fig. 3** Structures of bisaldehyde components **EG-ALD** and **$S_2$-ALD**.

**$S_2$-ALD** was prepared by the direct peptide coupling of cystamine with 4-formylbenzoic acid, mediated by *N'*-(3-dimethylaminopropyl)-*N*-ethylcarbodiimide (EDC) / 1-hydroxybenzotriazole (HOBt) (Scheme 2).

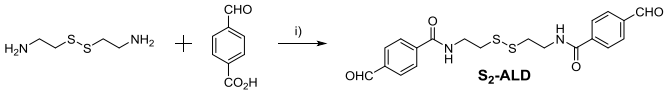


**Scheme 2** Synthesis of bisaldehyde **$S_2$-ALD**. Reagents and conditions: i) 4-formylbenzoic acid, EDC, HOBt, $Et_3N$, DMF, 0° to rt, 30% yield.

### Covalent self-assembly and formation of DCPs

We first carried out a model reaction to find suitable conditions in which both the acylhydrazone and the oxime reactions take place. We found that the addition of 2.0 equiv. of benzaldehyde to a 10 mM solution of **Ox-Arg-Hyd** in DMSO leads, after 48 hours at room temperature, to the complete conversion and formation of the expected product – identified by LCMS analysis (Fig. S35-S36) – that results from two condensation reactions.[76] The formation of DCPs was then engaged using these reaction conditions in DMSO as solvent. Since the concentration has a strong effect on the self-assembly because it affects the cycle–chain equilibria, the bisaldehyde and **Ox-AA-Hyd** building blocks were combined in stoichiometric amounts and studied at different concentrations.

MALDI-ToF mass spectrometry was used to characterize the self-assembled system, and the analysis of samples of **Poly(EG-Gly)**, **Poly(EG-Arg)** and **Poly(EG-His)**, prepared at 100 mM in DMSO, clearly shows the coexistence of cyclic and linear species (Fig. 4 and S37-S38).

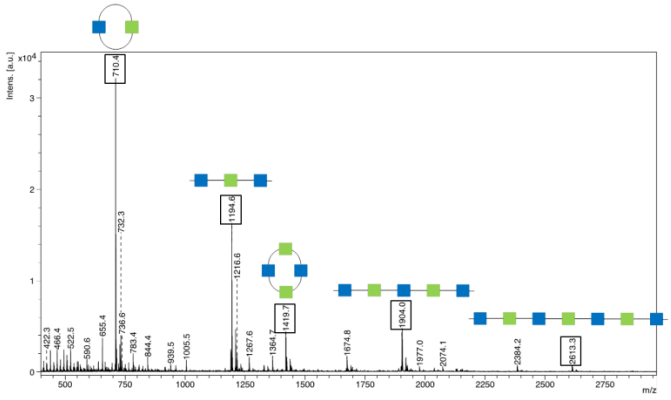


**Fig. 4** MALDI-TOF (HCCA matrix) mass spectrometry analysis of **Poly(EG-Arg)**, prepared by the self-assembly of **EG-ALD** and **Ox-Arg-Hyd** carried out at 100 mM in DMSO. Macrocycles and oligomers are schematically represented using alternate green and blue squares.

DOSY-NMR was then used to characterize the size of the species generated through this polycondensation self-assembly. The results confirm that small species, with hydrodynamic diameter similar to that of the initial building blocks, are formed at low concentration (typically 1-10 mM, Table 1). However, an unambiguous increase in size is observed as the concentration is raised (Table 1, Fig. S39-S47). Again, this is best explained by a shift in the cycle–chain equilibrium favoring open oligomers at high concentration.

**Table 1** Characterization of polycondensation reactions by DOSY-NMR. Hydrodynamic diameter were determined using the Stockes-Einstein equation.

| Entry | Compounds | Concentration (mM) | Diffusion coefficient ($m^2.s^{-1}$) | Hydrodynamic diameter (Å) |
|---|---|---|---|---|
| **1** | | 200 | $1.51 \times 10^{-11}$ | 146 |
| **2** | | 100 | $3.38 \times 10^{-11}$ | 64 |
| **3** | **Poly(EG-Arg)** | 50 | $4.17 \times 10^{-11}$ | 52 |
| **4** | | 10 | $6.88 \times 10^{-11}$ | 32 |
| **5** | | 1 | $1.31 \times 10^{-10}$ | 16 |
| **6** | | 200 | $2.87 \times 10^{-11}$ | 76 |
| **7** | | 100 | $4.9 \times 10^{-11}$ | 44 |
| **8** | **Poly(EG-His)** | 50 | $7.3 \times 10^{-11}$ | 30 |
| **9** | | 10 | $1.16 \times 10^{-10}$ | 18 |
| **10** | | 100 | $2,2 \times 10^{-11}$ | 100 |
| **11** | **Poly(EG-Gly)** | 50 | $4.2 \times 10^{-11}$ | 50 |
| **12** | | 10 | $6.3 \times 10^{-11}$ | 34 |

Finally, gel permeation chromatography of **Poly(EG-Gly)**, prepared at a concentration of 100 mM, confirms the presence of oligomers, yielding a value of $M_n$ = 2144 $g.mol^{-1}$ which amounts to a degree of polymerization DP = 7.0 (Fig. S48). The polydispersity is relatively high (Đ = 1.7) which is typical of step-growth polycondensations. Since GPC analysis was run at 60°C, we expect a faster conversion of the chains into smaller cyclic structures, therefore we take this value as an underestimate of the real size of the DCPs. Nevertheless we found that the hydrodynamic radii determined by DOSY-NMR correlates quite well with the molecular weight found using GPC. Indeed, the hydrodynamic radius is a function of the molecular weight – it varies as the square root or cubic root of the molecular weight, for rod or spherical shapes respectively.[77, 78] In our case, this calculation fits well with the rod model (comparison of **Poly(EG-Gly)** at 100 mM with its average monomer size: ratio of hydrodynamic radii for = 2.9; square root of molecular weight ratio = 2.6; cubic root of molecular weight ratio = 1.9).

The DCPs thus produced are therefore clearly oligomers, which is quite typical for polymers that are self-assembled under thermodynamic control. However, multivalent effects in DNA binding have been evidenced in different systems from rather low valency,[14, 35, 65, 79, 80] which indicate that our DCPs may have suitable degree of polymerization. We then engaged these novel DCPs, produced at 200 mM, in biological studies aiming at assessing their potential for DNA complexation and siRNA delivery. Using the same covalent self-assembly methodology, we also prepared, from the disulfide building block **$S_2$-ALD**, the double-degradable DCPs **Poly($S_2$-His)**, **Poly($S_2$-Arg)**, as well as the mixed DCP **Poly(EG-Arg-His)** containing 50 mol% of **Ox-Arg-Hyd** and 50 mol% of **Ox-His-Hyd** building block with respect to **EG-ALD**.

### DNA complexation

**Fluorescence assay**. The ability of the different DCPs to complex double stranded DNA (dsDNA) was assessed by a fluorescence displacement assay with calf thymus DNA (ctDNA) and ethidium bromide (EthBr) in aqueous buffer (pH = 7) at physiological saline conditions (150 mM NaCl). The principle of this assay is that fluorescence emission of EthBr at 590 nm increases upon intercalation into dsDNA and decreases upon addition of a DNA complexing agent which expels EthBr during the condensation of DNA into a nanoparticle. **Poly(EG-Arg)** and **Poly(EG-His)** were titrated onto a solution of ctDNA and EthBr and a significant decrease of the fluorescence emission was observed, which indicates that DNA complexation takes place (Fig. 5).[81] **Poly(EG-Arg)** was found to be superior to **Poly(EG-His)**, highlighting again the "Arginine magic" effect,[15] and achieves maximal complexation at N/P = 4, which is very good and similar to the typical N/P values recommended for transfection using commercial cationic polymers. In contrast, the building blocks **Ox-Arg-Hyd** and **Ox-His-Hyd** showed no fluorescence emission decrease (Fig. 5), therefore indicating the prime importance of multivalent interactions in DNA complexation.

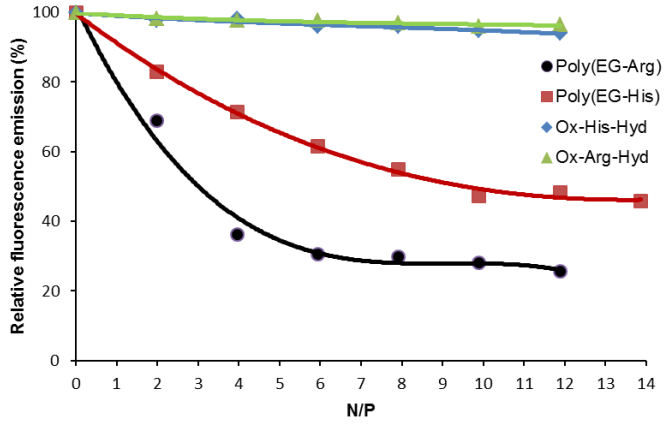


**Fig. 5** Fluorescence titration of a solution of calf thymus DNA and ethidium bromide by **Poly(EG-Arg)**, **Poly(EG-His)**, **Ox-Arg-Hyd**, and **Ox-His-Hyd** in HEPES buffer (100 mM, pH 7.0; 10 µM EDTA; 150 mM NaCl). The N/P value corresponds to the ratio of positive charges brought by the protonated nitrogens contained in the DCPs to the negative charges brought by the phosphodiesters of DNA.

**Gel electrophoresis**. Electrophoretic mobility shift assay (EMSA) was used to confirm the ability of these DCPs to complex dsDNA at pH=7. In this experiment we used a plasmid DNA (pDNA) and tested different N/P ratios (1 to 50). The results showed no shift of the plasmid band with **Poly(EG-Gly)** and **Poly(EG-His)** (Fig. 6). However, a strong retardation effect was observed using **Poly(EG-Arg)** with the complete disappearance of the band corresponding to the native plasmid at N/P ≥ 10 (Fig. 6). Thus, this result is in line with the previous fluorescence assay and confirms the superiority of **Poly(EG-Arg)**. Furthermore, the comparison with the monovalent cationic building block **Ox-Arg-Hyd**, which do not complex pDNA in the range of N/P = 20-300 (Fig. S49), demonstrate again the key role of multivalency. However, the absence of pDNA complexation by **Poly(EG-His)** was at first sight puzzling and in contradiction with the results of the fluorescence displacement assay. We hypothesized that the slightly basic pH used in the gel electrophoresis analysis (TAE buffer, pH = 8.2) would reduce the degree of protonation of this DCP and therefore weaken its interaction with pDNA. Indeed, when pDNA complexation was carried out at acidic pH (100 mM acetate buffer, pH = 5.0), gel electrophoresis analysis revealed again that **Poly(EG-His)** is capable of complexing pDNA from N/P ≥ 5 (Fig. S50). The DCPs containing disulfides exhibited the same trend, with **Poly($S_2$-Arg)** being superior (complexation at N/P > 5) than **Poly($S_2$-His)** (Fig. S51).

### siRNA complexation

**Gel electrophoresis.** The DCPs **Poly(EG-Arg)** and **Poly(Eg-His)** were also tested by gel electrophoresis at different N/P for their interaction with siRNA-Luc. The results show that both **Poly(EG-Arg)** and **Poly(Eg-His)** are able to non-covalently associate with siRNA at N/P > 2 were the band corresponding to free siRNA vanishes (Fig 7). These results confirm that the trend initially observed in DNA complexation holds also for siRNA complexation.

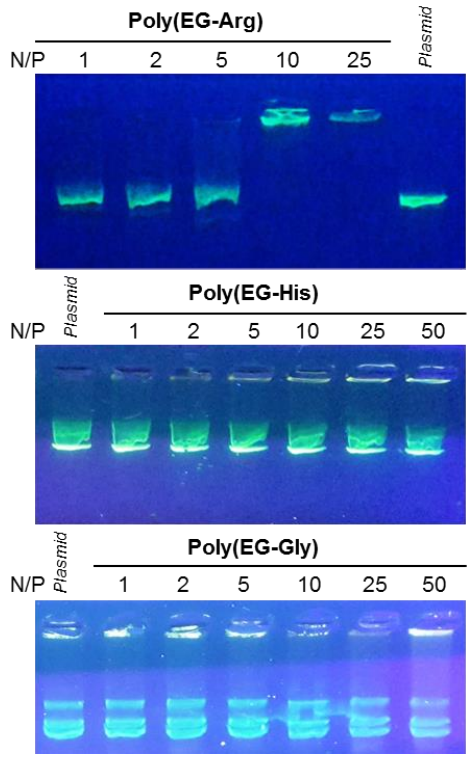


**Fig. 6** Gel electrophoresis of plasmid DNA with **Poly(EG-Arg)**, **Poly(EG-His)**, and **Poly(EG-Gly)** at different N/P. Note that in the case of the neutral DCP **Poly(EG-Gly)**, similar molar ratios were used for comparison with the cationic DCPs **Poly(EG-Arg)** and **Poly(EG-His)**.

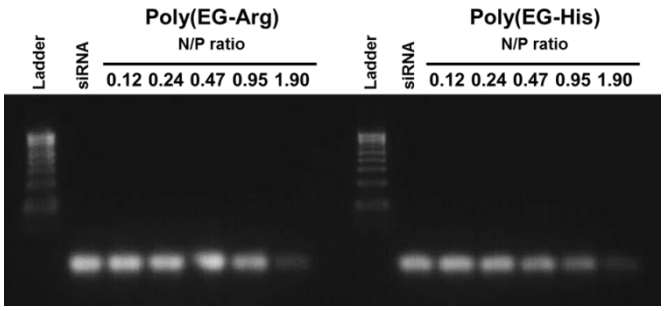


**Fig. 7** Gel retardation assay indicating the formation of DCP/siRNA complexes. DCPs **Poly(EG-Arg)** and **Poly(EG-His)** were added to a 21-mer siRNA at different N/P.

**ζ-potential**. We next monitored polyplexes formation by ζ-potential measurements. While siRNA alone has a negative ζ-potential of -19.9 mV (Table 2, entry 1), the addition of DCP **Poly(EG-Arg)**, which contains arginines, showed complexation through charge neutralization, the final polyplexes reaching a ζ-potential of 5.3 and 4.7 mV at N/P = 5.0 and 7.5, respectively (Table 2, entries 2-4). A similar trend was also observed with the other arginine-based DCP **Poly($S_2$-Arg)** (Table 2, entries 11-13). Confirming their lower ability to complex DNA and siRNA, the DCPs containing histidine derivatives showed less pronounced changes in ζ-potentials (Table 2, entries 5-7 and 14-16). Unfortunately, the mixed DCP **Poly(EG-Arg-His)** showed a similar behavior indicating weak siRNA complexation (Table 2, entries 5-7 and 8-10). It therefore seems that reducing the density of guanidinium groups by inserting lower

pKa building block into a polyarginine DCP reduces the "arginine magic" effect and weaken DNA/RNA complexation as proposed by Matile *et al*.[15]

**Dynamic light scattering**. The condensation of siRNA-Luc into nanoparticles, promoted by DCPs **Poly(EG-Arg)**, **Poly(EG-His)**, and **Poly(EG-Arg-His)** was then studied by dynamic light scattering experiments. A narrow distribution of particles was found using **Poly(EG-Arg)** at N/P = 2.5 (average diameter = 152.7 ± 0.8 nm; PDI = 0.27 ± 0.02) (Table 2, entry 2). Smaller nanoparticles were observed with **Poly(EG-His)** (average diameter = 72.7 ± 1.0 nm; PDI = 0.26 ± 0.01) (Table 2, entry 5). **Poly(EG-Arg-His)** forms slightly larger but more homogeneous nanoparticles (average diameter = 157.0 ± 6.3 nm; PDI = 0.17 ± 0.02) (Table 2, entry 8). However, testing larger N/P ratios (N/P = 5 and 7.5) led in all three cases to the formation of much larger nanoparticles (average diameters above 500 nm, see Table 2) unsuitable for cell entry through typical endocytosis pathways. Therefore, despite unfavorable ζ-potentials, the subsequent biological studies on these siRNA polyplexes have been carried out at N/P = 2.5 where siRNA complexation results in the formation of nanoparticles with suitable sizes for siRNA delivery.

**Table 2** Particle size, polydispersity index (PDI), and ζ-potential characterization by dynamic light scattering and ζ-potential measurements for the polyplexes formed upon addition of DCPs **Poly(EG-Arg)**, **Poly(EG-His)**, **Poly(EG-Arg-His)**, **Poly($S_2$-Arg)** and **Poly($S_2$-His)** onto siRNA in phosphate buffer (100 mM, pH=7). The values represent the average of three replicates.

| Entry | Compounds | N/P | ζ potential (mV) | Size / nm | PDI |
|---|---|---|---|---|---|
| **1** | **siRNA** | 0 | -19.9 | n.a. | n.a. |
| **2** | **Poly(EG-Arg)** | 2.5 | -8.9 | 152.7 ± 0.8 | 0.27 ± 0.02 |
| **3** | | 5 | 5.3 | 1033 ± 90 | 0.31 ± 0.04 |
| **4** | | 7.5 | 4.7 | 1777 ± 16 | 0.30 ± 0.03 |
| **5** | **Poly(EG-His)** | 2.5 | -19.8 | 72.7 ± 1.0 | 0.26 ± 0.01 |
| **6** | | 5 | -1.7 | 982 ± 93 | 0.26 ± 0.01 |
| **7** | | 7.5 | -1.6 | 1490 ± 62 | 0.33 ± 0.04 |
| **8** | **Poly(EG-Arg-His)** | 2.5 | -11.1 | 157.0 ± 6.3 | 0.17 ± 0.02 |
| **9** | | 5 | -4.7 | 347.5 ± 13.5 | 0.26 ± 0.01 |
| **10** | | 7.5 | -0.8 | 661.2 ± 40.9 | 0.25 ± 0.01 |
| **11** | **Poly($S_2$-Arg)** | 2.5 | -17.9 | n.d. | n.d. |
| **12** | | 5 | -6.4 | n.d. | n.d. |
| **13** | | 7.5 | -1.1 | n.d. | n.d. |
| **14** | **Poly($S_2$-His)** | 2.5 | -9.9 | n.d. | n.d. |
| **15** | | 5 | -9.9 | n.d. | n.d. |
| **16** | | 7.5 | -10.8 | n.d. | n.d. |

## Cell studies

**Cytotoxicity study**. This experiment is conducted on MCF7-Luc that is a cell line derived from MCF7 human breast cancer cells transfected by firefly luciferase gene, using the 21-mer siRNA 5'-AACUUACGCUGAGUACUUCGA-3' targeting the expression of luciferase. To analyze the cytotoxicity induced by the nanoparticles, MCF7-Luc cells were incubated 72 h with the polymers condensed with 3 different amounts of siRNA. Then, at the end of the incubation a MTT assay was realized to evaluate the cell death. The results indicate that **Poly(EG-His)** is the least toxic while **Poly(EG-Arg)** showed a similar cell viability than Lipofectamine (Fig. 8). The DCPs **Poly(EG-Arg-His)**, **Poly($S_2$-Arg)**, and **Poly($S_2$-His)** were found to be slightly more toxic than Lipofectamine at high dose.

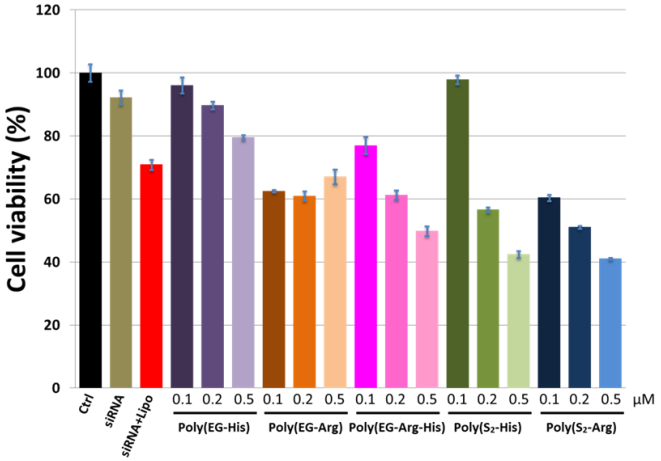


**Fig. 8** MTT cell viability assays on MCF7-Luc cells. The experiments were carried out with increasing amounts of siRNA (0.1 to 0.5 µM) at N/P = 2.5. The control experiment (Ctrl) corresponds to the MCF7-Luc cells without any treatment. The "siRNA" experiment corresponds to MCF7-Luc cells treated with naked siRNA. The "siRNA+Lipo" experiment corresponds to MCF7-Luc cells transfected with the complex Lipofectamine/siRNA. The results are expressed as mean ± standard deviation (*n*=3).

**siRNA delivery**. A luciferase assay was carried out on MCF7-Luc cell line, which is derived from MCF7 human breast cancer cells transfected by firefly luciferase gene, using the 21-mer siRNA 5'-AACUUACGCUGAGUACUUCGA-3' targeting the expression of luciferase. The results presented in Fig. 9 show a dose-dependent activity for all DCPs with **Poly(EG-Arg)** being the most effective vector – displaying an activity similar to Lipofectamine – whereas **Poly(EG-His)** is almost inactive. Given the results discussed above, the low activity of **Poly(EG-His)** can be understood by its low ability to complex siRNA and the negative ζ-potential of the corresponding polyplex which prevent the effective uptake and intracellular trafficking of the siRNA. Finally, although we could have expected a synergistic effect using the mixed DCPs **Poly($S_2$-Arg)** and **Poly($S_2$-His)** due to the presence of two complementary dynamics – pH-sensitive acylhydrazones and redox-sensitive disulfides – within their main chain, no significant improvements were observed experimentally. While **Poly($S_2$-His)** is indeed more effective than **Poly(EG-His)** at all doses, **Poly($S_2$-Arg)** performs equally well than **Poly(EG-Arg)** at 0.5 µM siRNA.

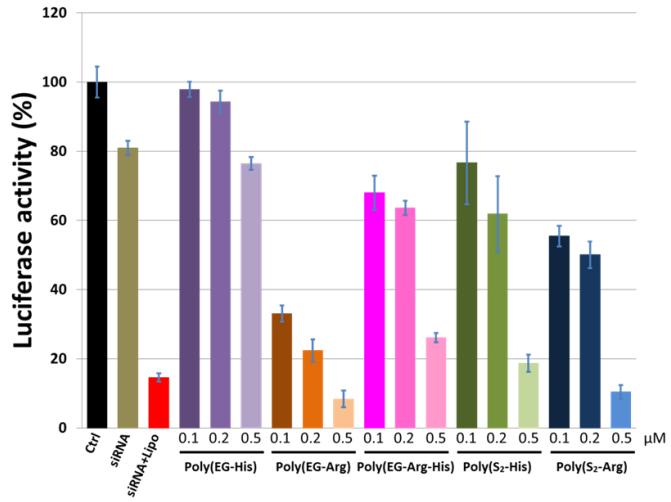


**Fig. 9** Luciferase activity assay showing the transfection of a 21-mer siRNA targeting the expression of luciferase inside MCF7-Luc. The experiments were carried out with increasing amounts of siRNA (0.1 to 0.5 µM) at N/P = 2.5. The control experiment (Ctrl) corresponds to the MCF7-Luc cells without any treatment. The "siRNA" experiment corresponds to MCF7-Luc cells treated with naked siRNA. The "siRNA+Lipo" experiment corresponds to MCF7-Luc cells transfected with the complex Lipofectamine/siRNA. The results are expressed as mean ± standard deviation (*n*=3).

## Conclusions

We have reported herein on the design and self-assembly of biomolecular dynamic covalent polymers (DCPs) for DNA complexation and siRNA delivery. These DCPs are self-produced through the reversible connection of amino acid derivatives featuring hydrazide and aminooxy groups at, respectively, the C- and N-termini with complementary bisaldehydes having ethylene glycol or disulfide spacers. The synthesis in solution of three modified amino acids – Gly, His, Arg – building blocks is disclosed here and the outcome of the covalent self-assembly process has been investigated in details by MALDI-ToF mass spectrometry, DOSY NMR spectroscopy, and GPC analysis. It is shown that the concentration affects cycle-chain equilibria and that oligomers of ca. 7 units are generated at 100 mM. DNA complexation by the cationic DCPs has been evidenced by fluorescence displacement assay and gel electrophoresis, both results showing the superiority of the arginine-based compared to the histidine-based DCPs. The successful extension of this initial approach to siRNA complexation has been achieved, demonstrating that these DCPs are effective siRNA complexing agents. Despite unfavorable ζ-potentials, the formation of nanoparticles of suitable sizes for siRNA delivery has been shown by dynamic light scattering experiments. Finally, biological studies reveal, through a luciferase assay, that the arginine-based DCP **Poly(EG-Arg)** can effectively deliver a functional siRNA in living cells. This unprecedented result represents a proof-of-concept for the application of DCPs in siRNA delivery. We believe that our straightforward and modular approach to the self-production of multifunctional and biomolecular DCPs as siRNA vectors will open new perspectives in smart gene delivery using dynamic and adaptive biodynamers.

## Experimental methods

Detailed materials and methods, synthetic protocols and additional characterization data can be found in the ESI online.

## Conflicts of interest

There are no conflicts to declare.

## Acknowledgements

We thank Aurelien Lebrun for DOSY NMR experiments, Dr. Benjamin Nottelet for GPC analyses, and Prof. Joël Chopineau for ζ-potential experiments. We acknowledge funding from the CNRS and the LabEx CheMISyst (ANR-10-LABX-05-01).

## References

1. C. F. Bennett and E. E. Swayze, *Annu. Rev. Pharmacol. Toxicol.*, 2010, **50**, 259-293.
2. E. Uhlmann and A. Peyman, *Chem. Rev.*, 1990, **90**, 543-584.
3. J. W. Gaynor, B. J. Campbell and R. Cosstick, *Chem. Soc. Rev.*, 2010, **39**, 4169-4184.
4. R. Barrangou and J. A. Doudna, *Nature Biotech.*, 2016, **34**, 933-941.
5. S. L. Ginn, I. E. Alexander, M. L. Edelstein, M. R. Abedi and J. Wixon, *J. Gene Med.*, 2013, **15**, 65-77.
6. C. Hinderer, N. Katz, E. L. Buza, C. Dyer, T. Goode, P. Bell, L. Richman and J. M. Wilson, *Hum. Gene Ther.*, 2018, **29**, DOI: 10.1089/hum.2018.1015.
7. U. Lächelt and E. Wagner, *Chem. Rev.*, 2015, **115**, 11043-11078.
8. H. Yin, R. L. Kanasty, A. A. Eltoukhy, A. J. Vegas, J. R. Dorkin and D. G. Anderson, *Nat Rev Genet*, 2014, **15**, 541-555.

9. M. A. Mintzer and E. E. Simanek, *Chem. Rev.*, 2009, **109**, 259-302.
10. S. K. Samal, M. Dash, S. V. Vlierberghe, D. L. Kaplan, E. Chiellini, C. v. Blitterswijk, L. Moroni and P. Dubruel, *Chem. Soc. Rev.*, 2012, **41**, 7147-7194.
11. H. T. Lv, S. B. Zhang, B. Wang, S. H. Cui and J. Yan, *J Control Release*, 2006, **114**, 100-109.
12. D. V. Schaffer, N. A. Fidelman, N. Dan and D. A. Lauffenburger, *Biotechnol. Bioeng.*, 2000, **67**, 598-606.
13. A. Fuertes, M. Juanes, J. R. Granja and J. Montenegro, *Chem. Commun.*, 2017, **53**, 7861-7871.
14. E. Bartolami, C. Bouillon, P. Dumy and S. Ulrich, *Chem. Commun.*, 2016, **52**, 4257-4273.
15. G. Gasparini, E.-K. Bang, J. Montenegro and S. Matile, *Chem. Commun.*, 2015, **51**, 10389-10402.
16. C. Alvarez-Lorenzo and A. Concheiro, *Chem. Commun.*, 2014, **50**, 7743-7765.
17. K. Miyata, N. Nishiyama and K. Kataoka, *Chem. Soc. Rev.*, 2012, **41**, 2562-2574.
18. Y. J. Kwon, *Acc. Chem. Res.*, 2012, **45**, 1077-1088.
19. E. Wagner, *Acc. Chem. Res.*, 2012, **45**, 1005-1013.
20. A. Barnard and D. K. Smith, *Angew. Chem. Int. Ed.*, 2012, **51**, 6572-6581.
21. A. Barnard, P. Posocco, S. Pricl, M. Calderon, R. Haag, M. E. Hwang, V. W. T. Shum, D. W. Pack and D. K. Smith, *J. Am. Chem. Soc.*, 2011, **133**, 20288-20300.
22. P. Posocco, S. Pricl, S. Jones, A. Barnard and D. K. Smith, *Chem Sci*, 2010, **1**, 393-404.
23. D. J. Welsh, S. P. Jones and D. K. Smith, *Angew. Chem. Int. Ed.*, 2009, **48**, 4047-4051.
24. M. A. Kostiainen, J. G. Hardy and D. K. Smith, *Angew. Chem. Int. Ed.*, 2005, **44**, 2556-2559.
25. S. Mukherjee, J. J. Cash and B. S. Sumerlin, in *Dynamic Covalent Chemistry: Principles, Reactions, and Applications*, eds. W. Zhang and Y. Jin, Wiley-VCH, Weinheim, 2017, pp. 321-358.
26. K. Imato and H. Otsuka, in *Dynamic Covalent Chemistry: Principles, Reactions, and Applications*, eds. W. Zhang and Y. Jin, Wiley-VCH, Weinheim, 2017, pp. 359-388.
27. F. Garcia and M. M. J. Smulders, *J. Polym. Sci., Part A: Polym. Chem.*, 2016, **54**, 3551-3577.
28. N. Roy, B. Bruchmann and J. M. Lehn, *Chem. Soc. Rev.*, 2015, **44**, 3786-3807.
29. J. M. Lehn, *Austr. J. Chem.*, 2010, **63**, 611-623.
30. T. Maeda, H. Otsuka and A. Takahara, *Prog. Polym. Sci.*, 2009, **34**, 581-604.
31. J.-M. Lehn, *Progr. Polym. Sci.*, 2005, **30**, 814-831.
32. R. Haag and F. Kratz, *Angew. Chem. Int. Ed.*, 2006, **45**, 1198-1215.
33. S. Son, R. Namgung, J. Kim, K. Singha and W. J. Kim, *Acc. Chem. Res.*, 2012, **45**, 1100-1112.
34. S. Bauhuber, C. Hozsa, M. Breunig and A. Gopferich, *Adv. Mater.*, 2009, **21**, 3286-3306.
35. M. A. Kostiainen and H. Rosilo, *Chem. Eur. J.*, 2009, **15**, 5656-5660.
36. S. Binauld and M. H. Stenzel, *Chem. Commun.*, 2013, **49**, 2082-2102.
37. A. Aissaoui, B. Martin, E. Kan, N. Oudrhiri, M. Hauchecorne, J. P. Vigneron, J.-M. Lehn and P. Lehn, *J. Med. Chem.*, 2004, **47**, 5210-5223.
38. P. Morelli, E. Bartolami, N. Sakai and S. Matile, *Helv. Chim. Acta*, 2018, **101**.
39. D. Abegg, G. Gasparini, D. G. Hoch, A. Shuster, E. Bartolami, S. Matile and A. Adibekian, *J. Am. Chem. Soc.*, 2017, **139**, 231-238.
40. L. L. Zong, E. Bartolami, D. Abegg, A. Adibekian, N. Sakai and S. Matile, *Acs Central Sci*, 2017, **3**, 449-453.
41. N. Chuard, G. Gasparini, A. Roux, N. Sakai and S. Matile, *Org. Biomol. Chem.*, 2015, **13**, 64-67.
42. G. Gasparini, G. Sargsyan, E. K. Bang, N. Sakai and S. Matile, *Angew. Chem. Int. Ed.*, 2015, **54**, 7328-7331.
43. E. K. Bang, S. Ward, G. Gasparini, N. Sakai and S. Matile, *Polym Chem-Uk*, 2014, **5**, 2433-2441.
44. G. Gasparini, E. K. Bang, G. Molinard, D. V. Tulumello, S. Ward, S. O. Kelley, A. Roux, N. Sakai and S. Matile, *J. Am. Chem. Soc.*, 2014, **136**, 6069-6074.
45. E. K. Bang, G. Gasparini, G. Molinard, A. Roux, N. Sakai and S. Matile, *J. Am. Chem. Soc.*, 2013, **135**, 2088-2091.
46. E. K. Bang, M. Lista, G. Sforazzini, N. Sakai and S. Matile, *Chem. Sci.*, 2012, **3**, 1752-1763.
47. P. K. Hashim, K. Okuro, S. Sasaki, Y. Hoashi and T. Aida, *J. Am. Chem. Soc.*, 2015, **137**, 15608-15611.
48. C. Bouillon, D. Paolantoni, J. C. Rote, Y. Bessin, L. W. Peterson, P. Dumy and S. Ulrich, *Chem. Eur. J.*, 2014, **20**, 14705-14714.
49. L. Marin, D. Ailincai, M. Cahn, D. Stan, C. A. Constantinescu, L. Ursu, F. Doroftei, M. Pinteala, B. C. Simionescu and M. Barboiu, *ACS Biomater. Sci. Eng.*, 2016, **2**, 104-111.
50. I. A. Turin-Moleavin, F. Doroftei, A. Coroaba, D. Peptanariu, M. Pinteala, A. Salic and M. Barboiu, *Org. Biomol. Chem.*, 2015, **13**, 9005-9011.
51. L. Clima, D. Peptanariu, M. Pinteala, A. Salic and M. Barboiu, *Chem. Commun.*, 2015, **51**, 17529-17531.
52. R. Catana, M. Barboiu, I. Moleavin, L. Clima, A. Rotaru, E.-L. Ursu and M. Pinteala, *Chem. Commun.*, 2015, **51**, 2021-2024.
53. I. Louzao, R. Garcia-Fandino and J. Montenegro, *J. Mater. Chem. B*, 2017, **5**, 4426-4434.
54. J. M. Priegue, D. N. Crisan, J. Martinez-Costas, J. R. Granja, F. Fernandez-Trillo and J. Montenegro, *Angew. Chem. Int. Ed.*, 2016, **55**, 7492-7495.
55. I. Lostale-Seijo, I. Louzao, M. Juanes and J. Montenegro, *Chem. Sci.*, 2017, **8**, 7923-7931.
56. B. Y. Shi, M. Zheng, W. Tao, R. Chung, D. Y. Jin, D. Ghaffari and O. C. Farokhzad, *Biomacromolecules*, 2017, **18**, 2231-2246.
57. E. Mastrobattista, M. A. E. M. van der Aa, W. E. Hennink and D. J. A. Crommelin, *Nat. Rev. Drug Discovery*, 2006, **5**, 115-121.
58. A. Barnard, P. Posocco, M. Fermeglia, A. Tschiche, M. Calderon, S. Pricl and D. K. Smith, *Org. Biomol. Chem.*, 2014, **12**, 446-455.
59. J. G. Hardy, C. S. Love, N. P. Gabrielson, D. W. Pack and D. K. Smith, *Org. Biomol. Chem.*, 2009, **7**, 789-793.

60. S. P. Jones, N. P. Gabrielson, D. W. Pack and D. K. Smith, *Chem. Commun.*, 2008, 4700-4702.
61. W. G. Skene and J.-M. P. Lehn, *Proc. Natl. Acad. Sci. USA*, 2004, **101**, 8270-8275.
62. J. Collins, Z. Y. Xiao, A. Espinosa-Gomez, B. P. Fors and L. A. Connal, *Polym. Chem.*, 2016, **7**, 2581-2588.
63. J. Collins, Z. Y. Xiao, M. Mullner and L. A. Connal, *Polym. Chem.*, 2016, **7**, 3812-3826.
64. A. Moulin, J. Martinez and J. A. Fehrentz, *J Pept Sci*, 2007, **13**, 1-15.
65. E. Bartolami, Y. Bessin, N. Bettache, M. Gary-Bobo, M. Garcia, P. Dumy and S. Ulrich, *Org. Biomol. Chem.*, 2015, **13**, 9427-9438.
66. J. B. Matson and S. I. Stupp, *Chem. Commun.*, 2011, **47**, 7962-7964.
67. Y. Liu, J. M. Lehn and A. K. H. Hirsch, *Acc. Chem. Res.*, 2017, **50**, 376-386.
68. D. K. Kölmel and E. T. Kool, *Chem. Rev.*, 2017, **117**, 10358-10376.
69. S. Ulrich, D. Boturyn, A. Marra, O. Renaudet and P. Dumy, *Chem. Eur. J.*, 2014, **20**, 34-41.
70. S. Hyun, Y. Choi, H. N. Lee, C. Lee, D. Oh, D.-K. Lee, C. Lee, Y. Lee and J. Yu, *Chem. Sci.*, 2018, **9**, 3820-3827.
71. Y. L. Cheng, R. C. Yumul and S. H. Pun, *Angew. Chem. Int. Ed.*, 2016, **55**, 12013-12017.
72. M. Ripoll, P. Neuberg, A. Kichler, N. Tounsi, A. Wagner and J. S. Remy, *ACS Appl. Mater. Interfaces*, 2016, **8**, 30665-30670.
73. A. Frere, M. Kawalec, S. Tempelaar, P. Peixoto, E. Hendrick, O. Peulen, B. Evrard, P. Dubois, L. Mespouille, D. Mottet and G. Piel, *Biomacromolecules*, 2015, **16**, 769-779.
74. E. Bertrand, C. Goncalves, L. Billiet, J. P. Gomez, C. Pichon, H. Cheradame, P. Midoux and P. Guegan, *Chem. Commun.*, 2011, **47**, 12547-12549.
75. D. Putnam, C. A. Gentry, D. W. Pack and R. Langer, *Proc. Natl. Acad. Sci. USA*, 2001, **98**, 1200-1205.
76. Two compounds, whose m/z values correspond to the product of a single condensation reaction, acylhydrazone or oxime, were observed at intermediate reaction times.
77. P. Timmerman, J. L. Weidmann, K. A. Jolliffe, L. J. Prins, D. N. Reinhoudt, S. Shinkai, L. Frish and Y. Cohen, *J. Chem. Soc., Perkin Trans. 2*, 2000, 2077-2089.
78. A. R. Waldeck, P. W. Kuchel, A. J. Lennon and B. E. Chapman, *Prog. Nucl. Magn. Reson. Spectrosc.*, 1997, **30**, 39-68.
79. E. Bartolami, Y. Bessin, V. Gervais, P. Dumy and S. Ulrich, *Angew. Chem. Int. Ed.*, 2015, **54**, 10183-10187.
80. M. Li, S. Schlesiger, S. K. Knauer and C. Schmuck, *Angew. Chem. Int. Ed.*, 2015, **54**, 2941-2944.
81. Poly(EG-Gly) could not be studied because of limited solubility in these conditions.